

Received: 2019.06.20

Accepted: 2019.08.22

Published: 2019.12.16

Long Noncoding RNA (lncRNA) FOXD2-AS1 Promotes Cell Proliferation and Metastasis in Hepatocellular Carcinoma by Regulating MiR-185/AKT Axis

Authors' Contribution:

Study Design A
Data Collection B
Statistical Analysis C
Data Interpretation D
Manuscript Preparation E
Literature Search F
Funds Collection G

BC 1 **Zheng Chen**
CD 2 **Zhen Zhang**
CD 1 **Dongbo Zhao**
DE 1 **Wei Feng**
EF 3 **Fanlai Meng**
DE 1 **Shihui Han**
CD 1 **Bin Lin**
AG 1 **Xin Shi**

1 Department of General Surgery, The Affiliated Suqian Hospital of Xuzhou Medical University, Suqian People's Hospital of Nanjing Drum Tower Hospital Group, Suqian, Jiangsu, P.R. China
2 Department of Anesthesiology, The Affiliated Suqian Hospital of Xuzhou Medical University, Suqian People's Hospital of Nanjing Drum Tower Hospital Group, Suqian, Jiangsu, P.R. China
3 Department of Pathology, The Affiliated Suqian Hospital of Xuzhou Medical University, Suqian People's Hospital of Nanjing Drum Tower Hospital Group, Suqian, Jiangsu, P.R. China

Corresponding Author: Xin Shi, e-mail: yangxiaowei0106@163.com

Source of support: This work was supported by the Suqian Science and Technology Support Project (social development grant no. S201618)

Background: The aim of this study was to investigate the effects and mechanisms of long noncoding (lnc) RNA FOXD2-AS1 in hepatocellular carcinoma development.


Material/Methods: Collecting the 3 pairs of adjacent and hepatocellular carcinoma tissue and analysis by gene chip. Evaluating the FOXD2-AS1 expression by *in situ* hybridization assay. Evaluating the FOXD2-AS1 to Bel-7402 biological activity *in vitro* study by Cell Counting Kit-8, flow cytometry, Transwell and wound healing assay and correlation between miR-185 by dual-luciferase reporter assay. The relative proteins expressions were evaluated by western blot assay.

Results: FOXD2-AS1 was significantly upregulation in hepatocellular carcinoma tissues. FOXD2-AS1 knockdown suppressed Bel-7401 cell biological activities (proliferation, invasion, and migration) with miR-185 overexpression and AKT depressing in cell expression.

Conclusions: LncRNA FOXD2-AS1 promoted hepatocellular carcinoma development by regulation miR-185/AKT axis.

MeSH Keywords: **Biological Transport, Active • MicroRNAs • Proto-Oncogene Proteins c-akt • RNA, Long Noncoding**

Full-text PDF: <https://www.medscimonit.com/abstract/index/idArt/918230>

 3612

 1

 9

 34



Background

Primary hepatocellular carcinoma (HCC) is one of the common malignant tumors, especially in males. Its etiology and pathogenesis are still unclear. At present, it is believed that primary HCC is related to viral hepatitis, cirrhosis, and aflatoxin, among which viral hepatitis, especially hepatitis B, is closely related to primary HCC, and is the primary cause of the onset of primary HCC. Surgical treatment is still the main method for primary HCC. However, most primary HCC are diagnosed in advanced stage and lost to the treatment opportunity of surgery. There is no effective treatment for advanced HCC [1,2]. Therefore, further study on the pathogenesis of HCC and search for the pathogenic factors in the course of HCC are of great significance to the research and development of drugs for the treatment of HCC.

With the rapid development of microarray technology and whole genome sequencing technology, a class of non-coding RNAs that are initially considered as transcriptional noise has become a research hotspot in recent years [3]. The discovery of non-coding RNAs provides new ideas for the mechanism of occurrence and development of tumors. Among them, long non-coding RNAs (lncRNAs) are a class of non-coding RNAs whose length of transcript is longer than 200 bases [4], accounting for more than 80% of non-coding RNAs [5]. lncRNAs regulate gene expression mainly from epigenetic regulation, transcriptional regulation, and post-transcriptional regulation [6]. Considering that the number, type, function, and mechanism of lncRNAs are much more abundant compared with microRNAs (miRNAs), and lncRNAs may be the core of RNA regulation, increasing studies have shown that lncRNAs have great research potential, can be used as markers for diagnosis and prognosis of tumors, and are likely to become new targets for treatment of tumors [7,8]. Meanwhile, some previous studies [9–12] reported that lncRNAs were closely correlation with miRNAs in cancer, and lncRNAs could regulate cancer development via regulation miRNAs expression.

In this study, valuable lncRNAs in HCC were firstly explored by screening and analyzing their differential expression profiles, and then their differential expressions in HCC tissues and adjacent normal tissues were confirmed by *in situ* hybridization (ISH). Subsequently, the specific mechanism of lncRNA FOXD2-AS1 in HCC cell lines was verified by experiments in molecular biology.

Material and Methods

Tissue samples

Tissues samples were obtained from patients at the Affiliated Hospital of Xuzhou Medical University and Suqian People's

Hospital: 3 pairs of primary HCC tissues and adjacent tissues more than 2.0 cm away from the tumors. All the patients received no radiotherapy or chemotherapy preoperatively. Postoperative specimens were pathologically diagnosed as primary HCC. The specimens were stored in a refrigerator at -80°C 10 minutes after isolation. Additionally, the HCC tissues and corresponding adjacent tissues of 10 patients with stage I–II HCC and 5 patients with stage III–IV undergoing surgery for primary HCC from January 2017 to December 2017 were collected. There were 10 males and 5 females, aging 54.45 ± 4.54 years. Inclusion criteria included no preoperative radiotherapy or chemotherapy, pathologically confirmed primary HCC and complete data. Exclusion criteria were as follows: patients refusing participation, patients suffering from other malignant tumors, and patients with severe heart, liver, or kidney diseases. Sample collection in this experiment was approved by the ethics committee of our hospital and we obtained informed consent from patients or their families.

Gene chips

lncRNA gene chips were provided by Boobang Biological Technology Co., Ltd. All the chips were Agilent Human lncRNA chips (4×180 K, Design ID: 062918, lncRNA probe, 46,506). Total RNA of the samples was quantified by NanoDrop ND-2000 (Thermo Scientific), and RNA integrity was detected by Agilent Bioanalyzer 2100 (Agilent Technologies). Standard processes of sample labeling, chip hybridization and elution of reference chip after RNA quality was qualified were as follows. First, total RNA was reverse transcribed into double-stranded cDNA and further synthesized into cRNA labeled with cyanine-3-CTP (Cy3). The labeled cRNA was hybridized with the chip, and the original images were obtained by scanning with Agilent Scanner G2505C (Agilent Technologies) after elution. The original images were processed, and the original data were extracted using Feature Extraction software (version 10.7.1.1, Agilent Technologies). Then, quantile and subsequent processing was performed using GeneSpring (version 12.5; Agilent Technologies).

In situ hybridization (ISH)

The *in situ* hybridization (ISH) kit was purchased from Boshide (Wuhan, China) and operated according to the instructions. Each tissue specimen was treated with 20- μL digoxin-labeled lncRNA FOXD2-AS1 probe. After dewaxing, the tissue specimens were treated with 0.2 mol/L HCl for 5 minutes, fixed with 4% poly-formaldehyde at room temperature for 10 minutes, treated with 4 $\mu\text{g}/\text{mL}$ protease K at 25°C for 20 minutes, washed twice in PBS containing 0.2% glycine, balanced in 4×SSC (saline-sodium citrate) buffer for 15 minutes, dripped with pre-hybrid solution (50% deionized formamide, 10% glucose sulfate, 1×Denhardt's buffer, 4×SSC, 10 mmol/L DTT (dithiothreitol), 1 mg/mL yeast tRNA), pre-hybridized in a thermostat at 42°C for 2 hours, added

with 100 μ L pre-heated denatured hybrid solution (containing probe with a final concentration of 1 mg/mL) after absorbing superfluous liquid, covered with glass slips, and incubated in a thermostat overnight at 42°C. After removing the glass slips, the specimens were washed with 4 \times SSC for 15 minutes twice, 1 \times SSC for 15 minutes twice, and TBST (0.1 mol/L Tris-HCl pH 7.5, 0.15 mol/L NaCl, 0.1% Tween-20) for 10 minutes twice. Then, the specimens were dripped with HRP-labeled anti-biotin antibodies (working concentration 1: 500), placed at 4°C for 12 hours, washed with TBST for 10 minutes twice, and developed by DAB staining. The stained cells were observed under a microscope. Integrated optical density (IOD) values of specimens in each group were analyzed using Image J.

Cells and culture

Normal human hepatocytes (L-02) and human HCC cell lines (HepG2, Huh-7, SMMC-7721, Bel-7402, and Hep3B) were purchased from the American Type Culture Collection (ATCC). HCC cells and human hepatic epithelial cells were routinely cultured in DMEM medium containing 10% fetal bovine serum (FBS) and 1% penicillin-streptomycin in a constant temperature incubator at 37°C with 5% CO₂. When cell confluence reached 70%~80%, passage is carried out.

Cell transfection

Small interfering RNAs (siRNAs), plasmids, or microRNA (miRNA) mimics were transfected into Bel-7402 cells using HiGene transfection reagent (Applygen, Changping, Beijing, China). FOXD2-AS1 inhibit siRNA (si-FOXD2-AS1), negative control siRNAs (NC-siRNA), and miRNA-185 simulates were designed and synthesized by Transheep Biotechnology (Suzhou, Jiangsu, China). FOXD2-AS1 overexpression plasmid (pcDNA3.1-FOXD2-AS1) was synthesized by BioTransduction Lab Co., Ltd. (Wuhan, Hubei, China).

Bel-7402 cells in logarithmic growth phase were digested with trypsin, and then the density was adjusted to 1 \times 10⁵ cell/mL by DMEM medium. Then, the cells were inoculated into 6-well plates, and 2 mL cell suspension was added into each hole, and then were cultured at 37°C and 5% CO₂ for 24 hours and then transfected. The method of transfection was referred to the instructions of Lipofectamine™ 2000 transfection reagent. After 48 hours of transfection, the next experiment was carried out.

Real-time quantitative polymerase chain reaction (RT-qPCR)

Cells were collected and total RNA was extracted from cultured cells by 1-step TRIzol. Subsequently, the extracted RNA was treated with DNA enzymes, and cDNA was prepared using 1 μ g RNA by reverse transcription. Then, 2 μ L reverse transcription

Table 1. Primer sequence.

Primer	Sequence
U6	F: 5'-GAGGCACAGCGGAACG-3'
	R: 5'-CTACCACATAGTCCAGG-3'
GAPDH	F: 5'-GGTGAAGGTCGGAGTCAACG-3'
	R: 5'-CAAAGTTGTCATGGATGTAGG-3'
FOXD2-AS1	F: 5'-CCGCGTAAGCCTCATAGAAG-3'
	R: 5'-GGGAGTAGGGTGAGGAAAGG-3'
miR-185	F: 5'-GGATTGGAGAGAAAGGCAG-3'
	R: 5'-GTGCAGGGTCCGAGGT-3'

products were collected for PCR, with U6 and GAPDH as internal references. The primer sequences are shown in Table 1. A final volume of 20 μ L was established, including 2 μ L reverse transcription products, 10 μ L SYBRGreenMix and 0.5 μ L upstream and 0.5 μ L downstream primers (10 μ mol/L). The thermal cycle for PCR was carried out at 95°C for 5 minutes, followed by denaturation at 94°C for 30 seconds, annealing at 60°C for 30 seconds, with a total of 45 cycles. The results were calculated using the 2^{- $\Delta\Delta$ CT} method.

Detection of proliferation of Bel-7402 cells by Cell Counting Kit-8 (CCK-8)

The cells in each group were diluted to 10% CCK-8 solution to prepare cell suspension with a concentration of 1 \times 10⁶/mL, which was then cultured in a constant temperature incubator at 37°C for 4 hours. Finally, the optical density (OD) at 450 nm was measured and the cell proliferation rate was calculated. CCK-8 kit was purchased from Nanjing Jiancheng Institute of Bioengineering.

Flow cytometry assay

After transfection for 48 hours, Bel-7402 cells from each group were digested by protease K to prepare single-cell suspension, with cell concentration adjusted to 1 \times 10⁶/mL and a final concentration of 70% by adding 95% precooled ethanol. Then, the cells were immobilized in an ice bath for 60 minutes, and then centrifuged at 1000 rev/minute for 10 minutes. After discarding ethanol, the cells were re-suspended with phosphate buffered saline (PBS). Propidium iodide (PI) staining solution was added to the final concentration of 50 μ g/mL and RNase to the final concentration of 10 μ g/mL, which was incubated at room temperature in the dark for 30 minutes. Apoptosis was analyzed by flow cytometry.

Detection of invasion of Bel-7402 cells by Transwell

Matrigel glue dissolved overnight at 4°C was diluted on ice with serum-free culture medium at a ratio of 1: 7. Transwell chambers with 8-µm microporous polycarbonate membranes were placed in a sterile 24-well plate to form upper and lower chambers. Matrigel glue (25 µL) was added into the upper chamber and the 24-well plate was shaken quickly, so that the cells were evenly spread on the bottom of the chamber to avoid bubbles. The upper chamber was kept sterile overnight at 37°C to ensure the full polymerization of Matrigel glue. Cells were collected from each group. After culturing for 24 hours, the cells were digested with trypsin, single-cell suspension was prepared, and the cells were counted. The cells of each group were respectively added into the upper Transwell chamber (1.5×10^5 cells/chamber), and 650 µL DMEM (Dulbecco's Modified Eagle Medium) containing 10% FBS was added into the lower chamber. The cells were cultured routinely for 48 hours, and cells in the upper chamber were wiped with cotton swabs. After washing with PBS (3 times), the cells were stained with 0.1% crystal violet for 20 minutes and observed and photographed under an inverted phase-contrast microscope (200×). Five visual fields were observed randomly, and the number of membrane-penetrating cells was counted.

Detection of migration of Bel-7402 cells by wound healing

The cells in each group were prepared into cell suspension (100 µL) with cell density of 1×10^6 /mL, which was added into a 6-well plate and cultured overnight to form monolayer cells. Horizontal lines were drawn on monolayer cells using a 10-µL gun head, followed by washing with PBS 3 times to remove the exfoliated cells. Scratch widths were photographed and recorded under a microscope as the initial scratch widths. After culturing for 8 hours, the scratch widths were photographed and recorded again under the microscope. Scratch-healing rate=(initial scratch width–scratch width after 48-hour culture)/initial scratch width×100%.

Detection of AKT protein expression by western blotting

After cell transfection for 48 hours, the culture medium was discarded and rinsed gently with cold PBS once, then cold cell lysate was added to lyse the cells. The cells were scraped off and placed in an Eppendorf tube. The cells were repeatedly beaten 3 times with a cell membrane breaker to shear the nucleic acid in the cells, so that the protein was fully dissolved. The supernatant was centrifuged at 12 000 rev/minute and 4°C for 15 minutes. The supernatant was removed and transferred to another Eppendorf tube, then a fourth of the volume of 5 sample buffer was added, and then boiled for 10 minutes. The supernatant was stored at –20°C.

The protein concentration was determined according to the instructions of the diquinoline formic acid kit. Adding the 30 µg to each lane of a 10% polyacrylamide gel to separate proteins. The voltage of gel electrophoresis was controlled at 80–120 V, and the pressure of wet transport and transmembrane was controlled at 100 mV, lasting 45 to 70 minutes. After transmembrane with polyvinylidene fluoride, the protein was sealed in 5% bovine serum albumin for 1 hour, and then we added AKT (1: 500) and GAPDH (1: 1000) primary antibodies which were dilution by TBST for incubation at 4°C overnight. The protein was washed with membrane-washing buffer 3 times (5 minutes per time), followed by the addition of secondary antibodies and incubation at room temperature for 1 hour. After another washing of the membrane for 3 times, chemiluminescence reagent was added for the development of the proteins. With GAPDH as internal reference, the proteins were developed using Bio-Rad Gel DoleZ imager, and the gray level of the target protein band was analyzed using ImageJ software.

Cellular immunofluorescence

Bel-7402 cells from each group including NC, si-FOX2-AS1, miR-185, and pcDNA3.1-FOX2-AS1+miR-185 groups were cultured in 0.5% FBS medium for 24 hours after removing the supernatant, and serum-free DMEM medium was added into the control group. The expression of p-AKT in Bel-7402 cells was detected by immunofluorescence staining. Cell slides were fixed with 10% neutral formaldehyde solution, permeated with 0.25% Triton X-100 at room temperature for 10 minutes, and blocked with normal goat serum at room temperature for 30 minutes for non-specific reaction. Then, rabbit anti-human p-AKT primary antibody (1: 100) was added for incubation overnight at 4°C. After washing with PBS for 15 minutes 3 times, fluorescein isothiocyanate (FITC)-labeled sheep anti-rabbit secondary antibody was added for incubation at room temperature for 2 hours, and the nuclei were restained with DAPI (4',6-diamidino-2-phenylindole). The slides were sealed with glycerol, which were observed and photographed under confocal microscopy. Fluorescent staining results were quantitatively analyzed.

Dual-luciferase reporter assay

Using dual-luciferase reporter assay kit which were purchased from X-Y Biotechnology (Minhang, Shanghai, China). Synbio Technology Co., Ltd. (Suzhou, Jiangsu, China) constructed AKT wild-type 3'UTR (WT) plasmids and AKT mutant 3'UTR (MUT) plasmids.

Statistical processing

Using SPSS 20.0, all experiments were repeated 3 times independently. Measurement data were expressed in mean±standard

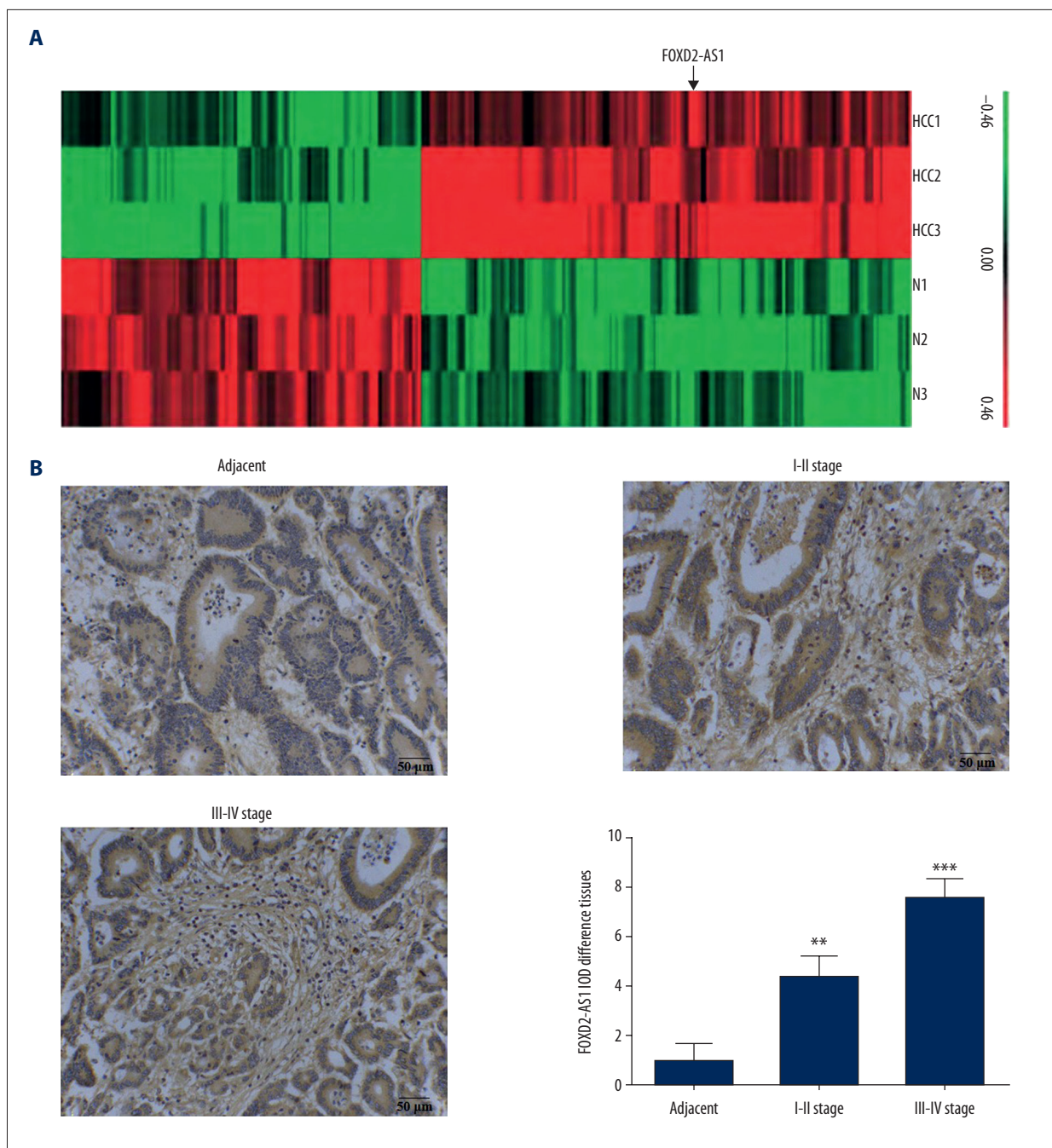


Figure 1. The clinical data and analysis. **(A)** Heat map of HCC. **(B)** LncRNA FOXD2-AS1 expression in difference tissues by ISH (200×). ** $P < 0.01$; *** $P < 0.001$ compared with adjacent normal tissues. HCC – hepatocellular carcinoma; lncRNA – long noncoding RNA; ISH – *in situ* hybridization.

deviations (SD). The means between 2 groups were compared using the *t*-test, and the data among multiple groups were compared with one-way ANOVA. The related pictures of the experimental data were drawn using GraphPad Prism 7. $P < 0.05$ or $P < 0.01$ was considered as statistically significant.

Results

LncRNA microarray and ISH in HCC and adjacent normal tissues

The expression of lncRNA in HCC tissues was significantly different from that in adjacent normal tissues. Based on differential

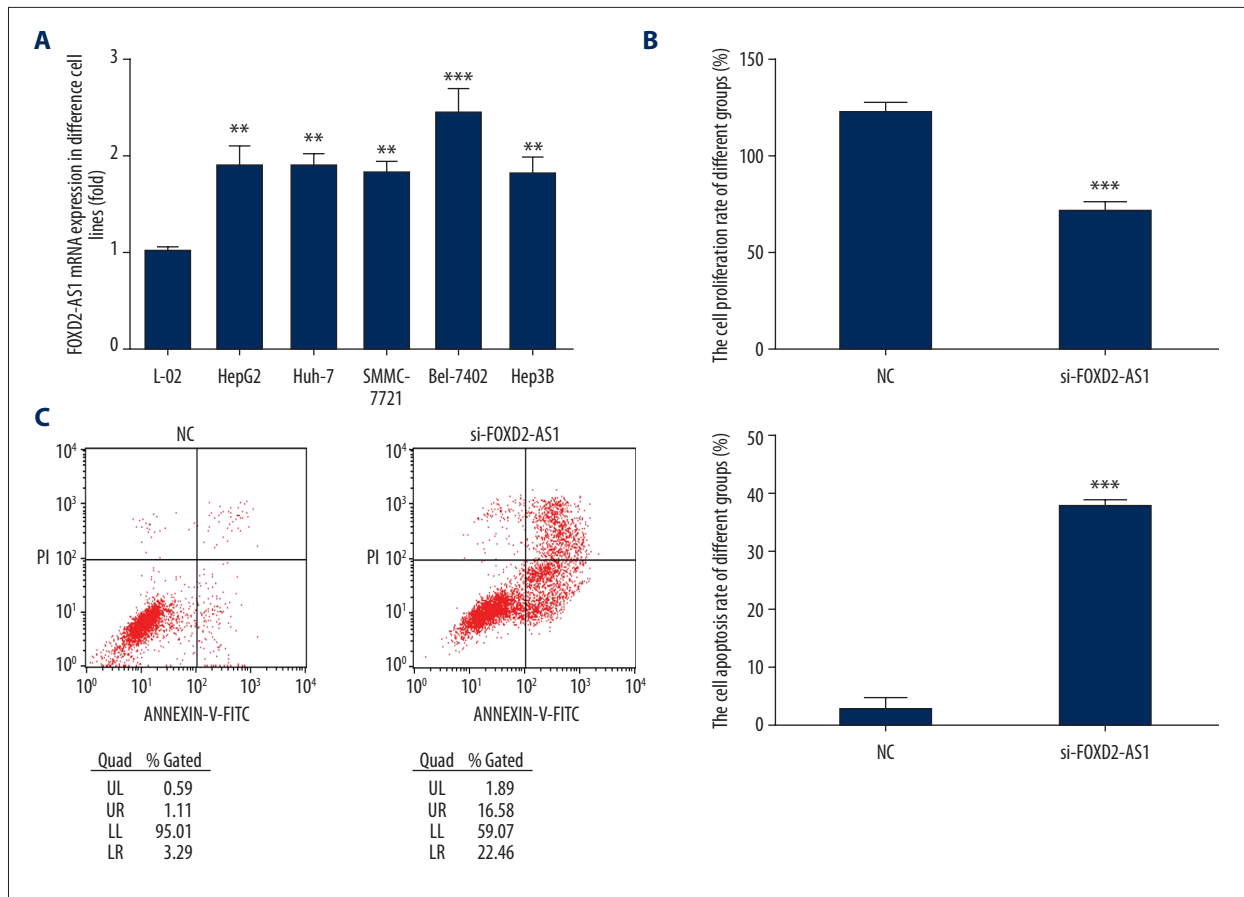


Figure 2. FOXD2-AS1 expression in difference cell lines and FOXD2-AS1 knockdown to cell proliferation and apoptosis. **(A)** FOXD2-AS1 mRNA expression in difference cell lines. ** $P < 0.01$, *** $P < 0.001$, compared with L-02 cell. **(B)** FOXD2-AS1 knockdown affects Bel-7402 cell proliferation. *** $P < 0.001$, compared with NC. **(C)** FOXD2-AS1 knockdown affects Bel-7402 cell apoptosis. *** $P < 0.001$, compared with NC.

multiples ≥ 2.0 and $P \leq 0.05$, a total of 182 differentially expressed lncRNAs with statistically significant difference were screened out in HCC tissues. Hierarchical clustering analysis showed that the differential expression profiles were reliable (Figure 1A). Among them, lncRNA FOXD2-AS1 presented the greatest difference. The expression of FOXD2-AS1 in HCC and adjacent normal tissues was detected by ISH, showing that the expression level of FOXD2-AS1 in HCC tissues was significantly higher than that in adjacent normal tissues ($P < 0.01$ or $P < 0.001$, respectively, Figure 1B). The expression of FOXD2-AS1 in stage III-IV HCC tissues was higher than that in stage I-II HCC tissues.

FOXD2-AS1 expression in normal hepatocytes and HCC cells and its effect on proliferation and apoptosis of HCC cells

Compared with normal hepatocytes (L-02), the expression of FOXD2-AS1 in HCC cell lines (HepG2, Huh-7, SMMC-7721, Bel-7402, and Hep3B) increased significantly ($P < 0.01$ or $P < 0.001$, respectively, Figure 2A). The mRNA expression of FOXD2-AS1

was the highest in HCC cell line Bel-7402. Therefore, Bel-7402 was used as the subject in this study. After knocking out FOXD2-AS1, compared with the NC group, the cell proliferation rate in the si-FOXD2-AS1 group decreased significantly and the apoptotic rate increased significantly ($P < 0.001$, respectively, Figure 2B, 2C).

Effects of FOXD2-AS1 knockout on invasion and migration of Bel-7402 cells

The effects of FOXD2-AS1 on the invasion and migration of Bel-7402 cells were investigated using Transwell and wound healing, respectively. Compared with the NC group, the number of invasive cells and wound healing rate in the si-FOXD2-AS1 group decreased significantly ($P < 0.001$, respectively, Figure 3A, 3B).

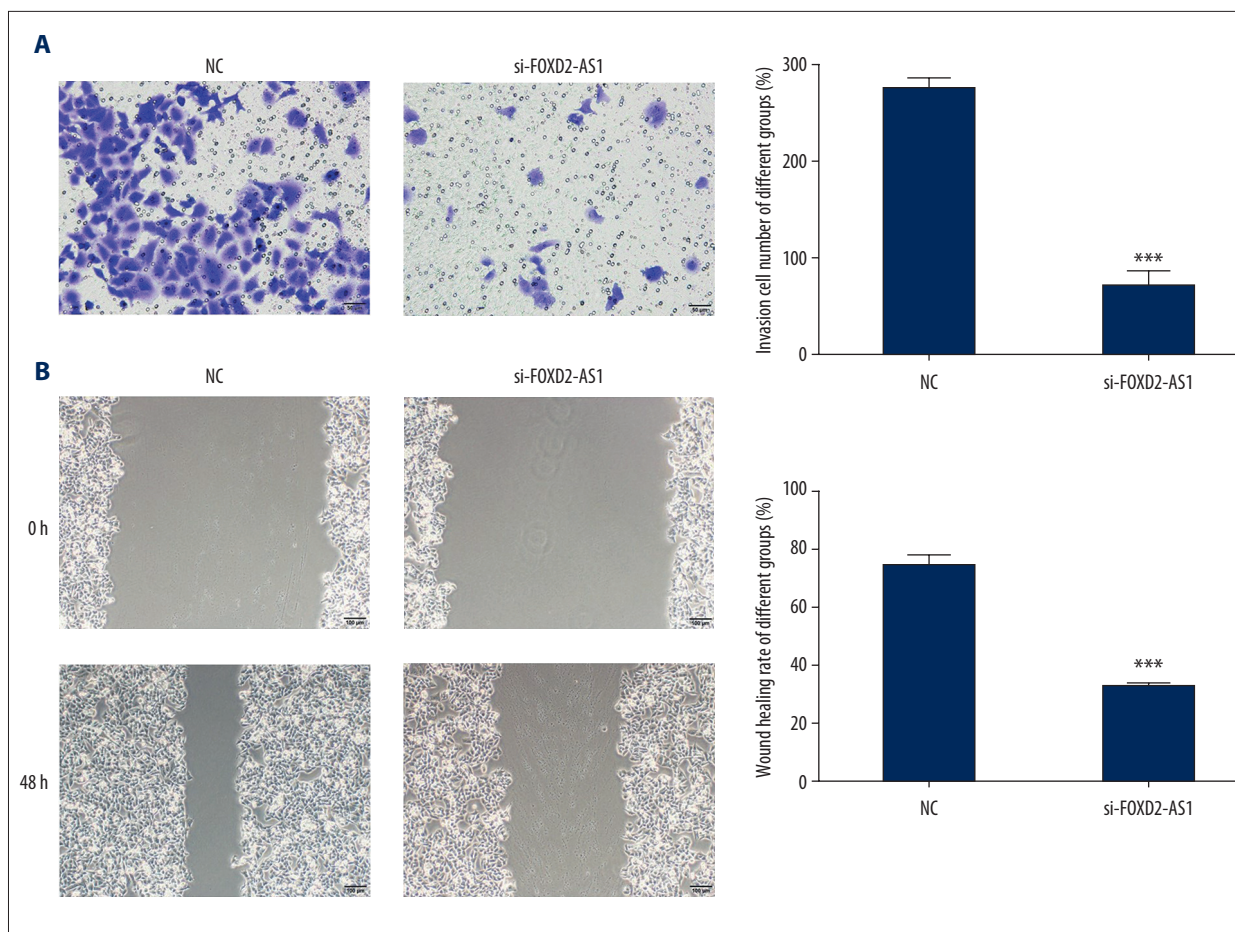


Figure 3. FOXD2-AS1 knockdown affects to cell invasion and migration in Bel-7402 cell line. **(A)** FOXD2-AS1 knockdown affects to cell invasion by Transwell assay (200 \times). *** $P < 0.001$ compared with NC group. **(B)** FOXD2-AS1 knockdown affects to cell migration by wound healing assay (100 \times). *** $P < 0.001$ compared with NC group.

Expression of miR-185 and its correlation with FOXD2-AS1

Compared with the NC group, the expression of miR-185 in the si-FOXD2-AS1 group increased significantly ($P < 0.001$, Figure 4A). The correlation between miR-185 and FOXD2-AS1 was investigated by dual-luciferase reporter assay. The results revealed that FOXD2-AS1 could target and regulate the expression of miR-185 in Bel-7402 cells ($P < 0.001$, Figure 4B).

Effects of FOXD2-AS1 knockout on AKT protein and p-AKT entering nuclei

Western blot results demonstrated that the expression of AKT protein was significantly inhibited after FOXD2-AS1 knockout ($P < 0.001$, Figure 5A) compared with the NC group. Cellular immunofluorescence assay showed that the number of p-AKT protein entering nuclei in the si-FOXD2-AS1 group with FOXD2-AS1 knockout was significantly lower than that in the NC group ($P < 0.001$, respectively, Figure 5B).

Effects of FOXD2-AS1 on proliferation and apoptosis of Bel-7402 cells via miR-185

After miR-185 was transfected into Bel-7402 cells, compared with the NC group, the proliferation rate of Bel-7402 cells decreased significantly ($P < 0.001$, Figure 6A) and the apoptotic rate increased significantly ($P < 0.001$, Figure 6B). However, after simultaneous transfection with FOXD2-AS1 and miR-185, the inhibitory effect of miR-185 on the proliferation and the promoting effect on the apoptosis of Bel-7402 cells were significantly inhibited. Compared with the miR-185 group, the proliferation rate of Bel-7402 cells in the pcDNA3.1-FOXD2-AS1+miR-185 group increased significantly ($P < 0.01$, Figure 6A) and the apoptotic rate was significantly inhibited ($P < 0.01$, Figure 6B).

Effects of FOXD2-AS1 on invasion and migration of Bel-7402 cells via miR-185

Compared with the NC group, the number of invasive Bel-7402 cells and wound healing rate were significantly inhibited after

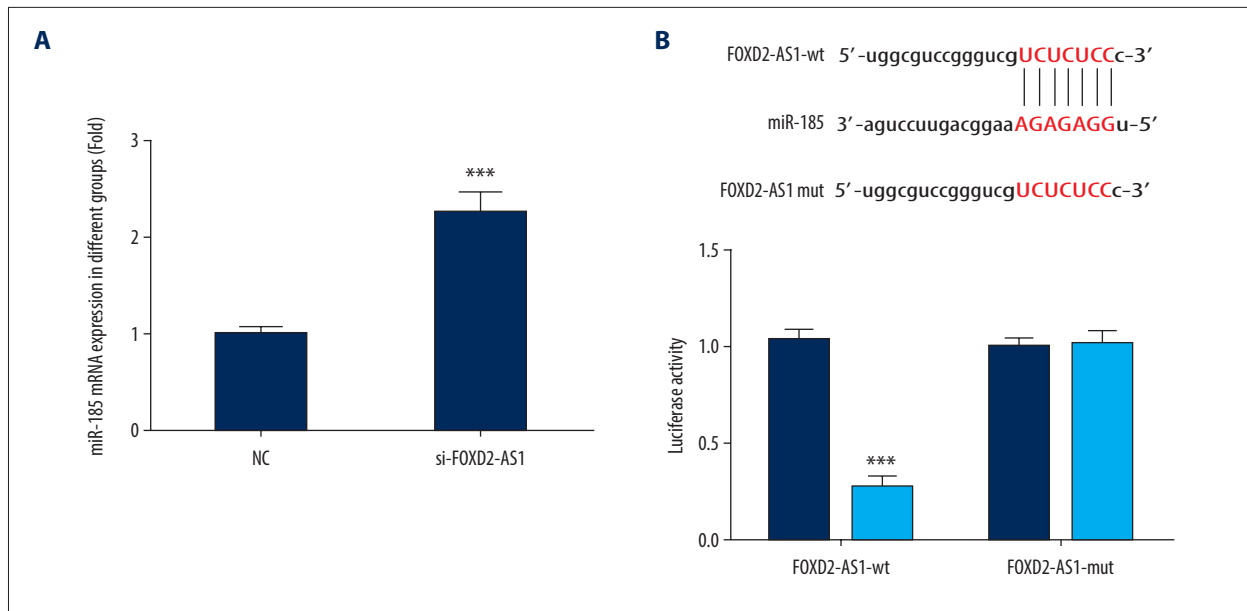


Figure 4. MiR-185 mRNA expression and correlation between FOXD2-AS1 and miR-185. **(A)** FOXD2-AS1 mRNA expression of difference groups. *** $P < 0.001$ compared with NC group. **(B)** Correlation between FOXD2-AS1 and miR-185. *** $P < 0.001$ compared with miR-NC group.

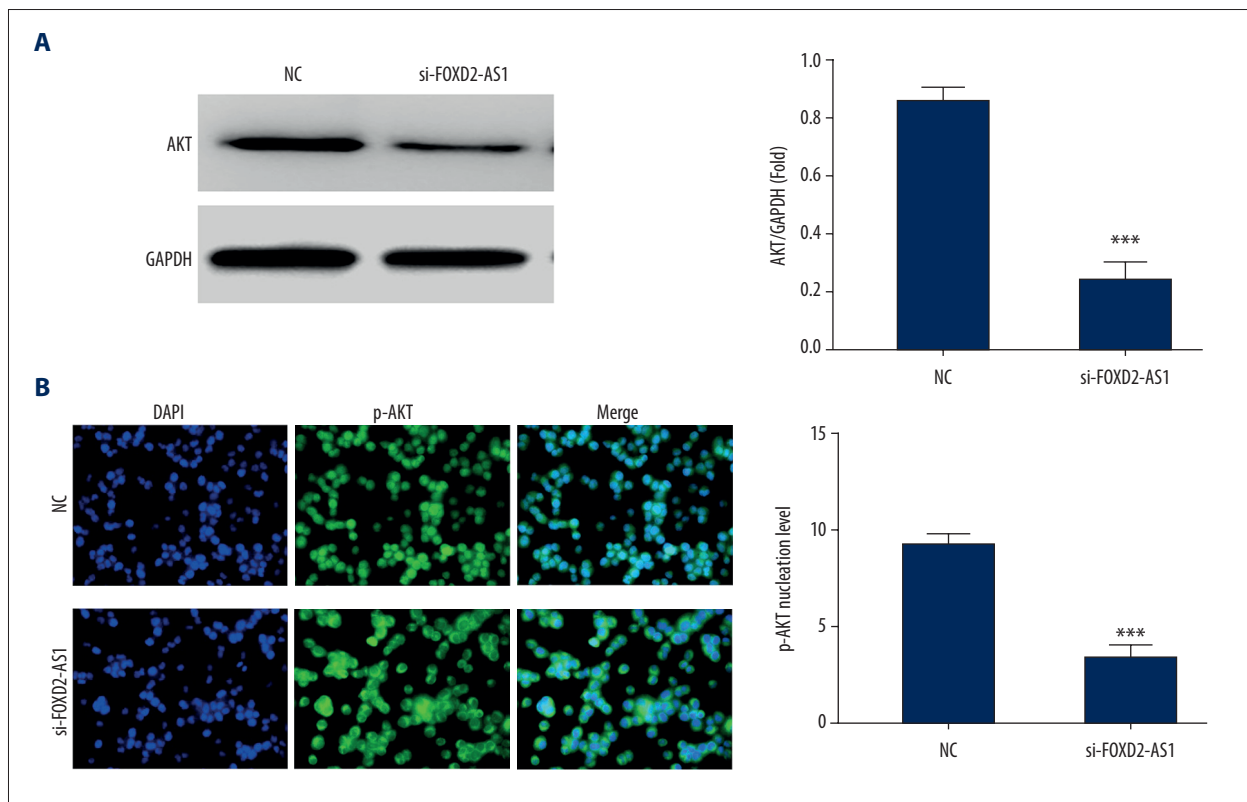


Figure 5. AKT and p-AKT protein express in difference groups. **(A)** AKT protein expression in difference groups by western blot assay. *** $P < 0.001$ compared with NC group. **(B)** p-AKT protein nuclear volume of difference groups by cellular immunofluorescence. *** $P < 0.001$ compared with NC group.

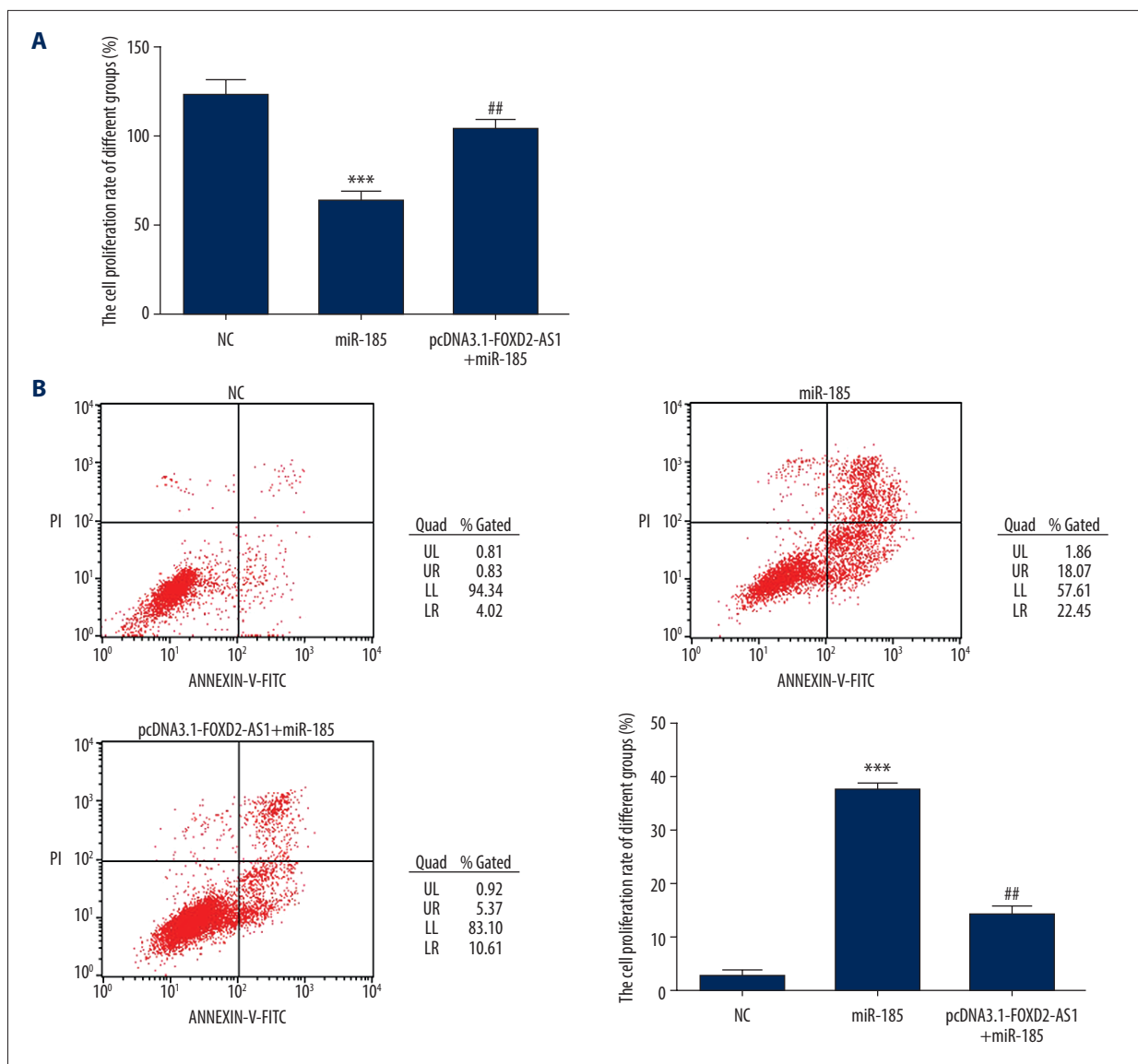


Figure 6. Cell proliferation and apoptosis in difference groups. (A) The cell proliferation of difference groups by Cell Counting Kit-8 assay. *** $P < 0.001$ compared with NC group; ** $P < 0.01$, compared with miR-185 group. (B) The cell apoptosis rate of difference groups by flow cytometry assay. *** $P < 0.001$ compared with NC group; ** $P < 0.01$, compared with miR-185 group.

miR-185 was transfected into Bel-7402 cells ($P < 0.001$, respectively, Figure 7A, 7B). After simultaneous transfection with FOXD2-AS1 and miR-185, the invasion and migration abilities of Bel-7402 cells in the pcDNA3.1-FOXD2-AS1+miR-185 group were significantly restored compared with the miR-185 group ($P < 0.01$, respectively, Figure 7A, 7B).

MiR-185 targeting and regulating AKT

Dual-luciferase reporter assay confirmed that in Bel-7402 cells, the expression of AKT was targeted and regulated by miR-185, as seen in Figure 8.

Effects of FOXD2-AS1 on AKT protein and p-AKT entering nuclei via miR-185

The results (Figure 9A) showed that the expression of AKT protein was significantly inhibited in the miR-185 group compared with the NC group ($P < 0.001$). After simultaneous transfection with FOXD2-AS1 and miR-185, the expression of AKT protein in the pcDNA3.1-FOXD2-AS1+miR-185 group increased significantly compared with the miR-185 group ($P < 0.01$, Figure 9A). Cellular immunofluorescence assay showed that compared with the NC group, the number of p-AKT protein entering nuclei was significantly inhibited in the miR-185 group ($P < 0.001$, Figure 9B). After simultaneous transfection with FOXD2-AS1

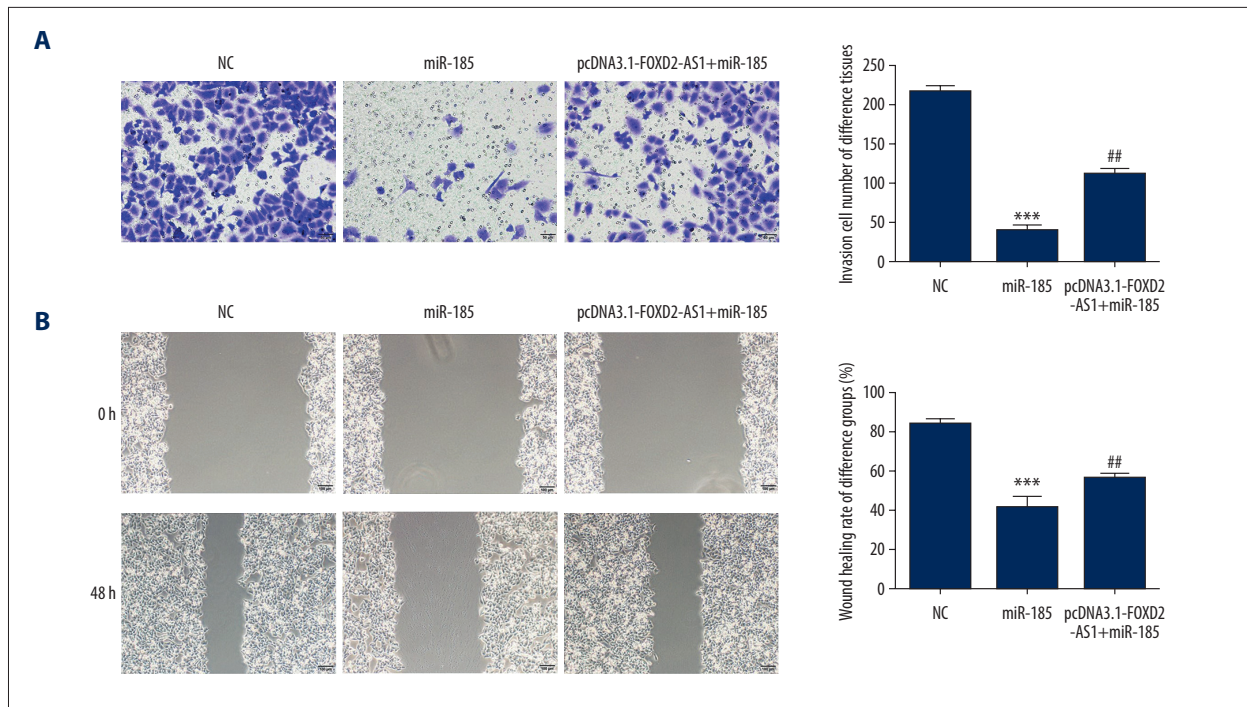


Figure 7. Cell invasion and migration in difference groups. **(A)** The invasion cell number of difference groups by Transwell assay (200×). *** $P < 0.001$ compared with NC group; ** $P < 0.01$, compared with miR-185 group. **(B)** The wound healing rate of difference groups by wound healing assay (100×). *** $P < 0.001$ compared with NC group; ** $P < 0.01$, compared with miR-185 group.

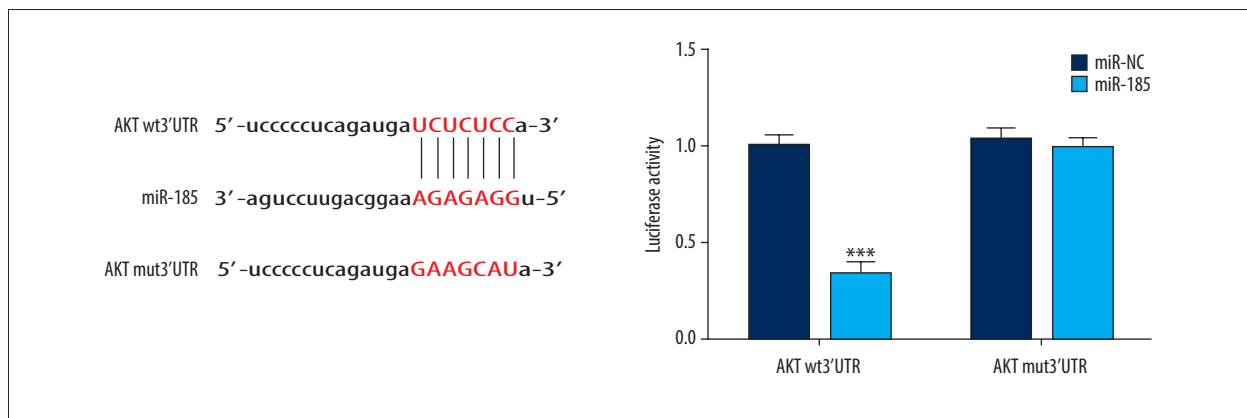


Figure 8. The correlation between miRNA-185 and AKT by dual-luciferase reporter assay. *** $P < 0.001$ compared with miR-NC.

and miR-185, the number of p-AKT protein entering nuclei in the pcDNA3.1-FOXD2-AS1+miR-185 group increased significantly compared with the miR-185 group ($P < 0.01$, Figure 9B).

Discussion

With the development of next-generation sequencing technologies, abnormal transcription and expression of more oncogenes have been found, including some non-coding RNAs, to which lncRNAs belong [13]. lncRNAs are a class of non-coding RNAs whose length exceeds 200 nt, without a complete open reading

frame or the ability to encode proteins. Most lncRNAs are transcribed from RNA polymerase II [14]. In recent years, increasing evidence demonstrate that these lncRNAs can be widely involved in genome regulation, regulating individual growth and development as well as cell apoptosis, proliferation and differentiation [15]. Moreover, they have been proven to be closely related to the occurrence and development of multiple malignant tumors, and can be used as specific markers of some malignant tumors and regulate the invasive and proliferative abilities of tumor cells. They play an important role in the occurrence, development, and prognosis of tumors. They are also closely related to the long-term prognosis of patients with malignant tumors [16,17].

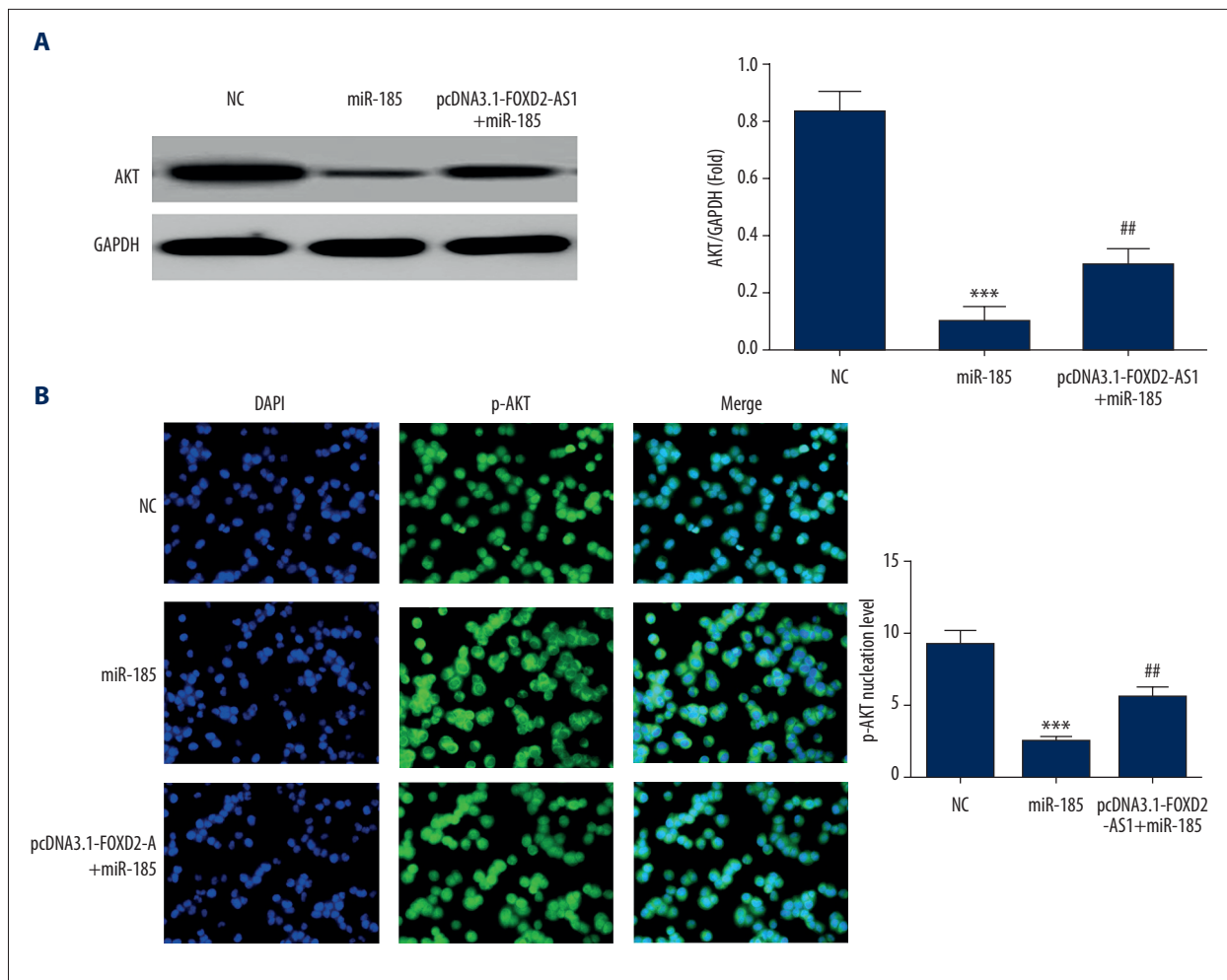


Figure 9. AKT and p-AKT proteins expression in difference groups. **(A)** AKT protein expression in difference groups by western blot assay. *** $P < 0.001$ compared with NC group; ** $P < 0.01$, compared with miR-185 group. **(B)** p-AKT protein nuclear volume in difference groups by cellular immunofluorescence. *** $P < 0.001$ compared with NC group; ** $P < 0.01$, compared with miR-185 group.

In recent years, in addition to structural noncoding RNAs and various microRNA (miRNAs), researchers have also found a class of lncRNAs with a length greater than 200 nucleotides. Although lncRNAs generally contain some conserved sequences, they regulate gene expression in various ways, including epigenetic regulation, transcriptional regulation and post-transcriptional regulation. In a word, lncRNAs regulate the occurrence and development of gastric cancer, thyroid cancer, colon cancer, and liver cancer by participating in many biological mechanisms such as X chromosome inactivation, genomic imprinting and DNA damage response [18]. Recent reports have presented that lncRNA MT1JP [19], lncRNA AFAP1 [20], and lncRNA SNHG8 [21] have significant effects on the proliferation, migration, and epithelial-mesenchymal transformation of tumor cells, suggesting that lncRNAs may be closely related to the occurrence and development of tumors. However, the specific molecular mechanism of lncRNA

FOXD2-AS1 in HCC cells is still unclear [22–24]. In this study, the differential expression of lncRNAs in 3 pairs of HCC and adjacent normal tissues was detected by gene chip technology and verified by ISH. The results showed that the expression of lncRNA FOXD2-AS1 in HCC tissues was high and correlated with the malignant degree of the tumor. In subsequent cell experiments, FOXD2-AS1 was knocked out in HCC cell line Bel-7402, revealing that the proliferation, invasion and migration of Bel-7402 cells were significantly inhibited.

Recent studies have found that the abnormal regulation of miRNAs is considered to be a key factor in the occurrence and development of many diseases, including gastric cancer. For instance, miR-185 inhibits the proliferation and migration of tumors by downregulating the expression of TRIM29 [25]. Moreover, studies have shown that miR-185 has significant effects on the proliferation, migration, and

epithelial-mesenchymal transformation of gastric cancer [26], lung cancer [27], colon cancer [28], pancreatic cancer [29], and liver cancer [30]. Some previous studies [31,32] found AKT was the target gene of miR-185 in some cell lines. Meanwhile, in this study, dual-luciferase reporter assay confirmed that miR-185 was the target site of FOXD2-AS1 and AKT was the target site of miR-185. The activation of AKT and the increase in the number p-AKT protein entering nuclei are important factors leading to the enhancement of cancer cell activity [33,34].

References:

1. Crocetti L, Bargellini I, Cioni R: Loco-regional treatment of HCC: Current status. *Clin Radiol*, 2017; 72(8): 626–35
2. Cong WM, Wu MC: New insights into molecular diagnostic pathology of primary liver cancer: Advances and challenges. *Cancer Lett*, 2015; 368(1): 14–19
3. Derrien T, Johnson R, Bussett G et al: The GENCODE v7 catalog of human long noncoding RNAs: Analysis of their gene structure, evolution, and expression. *Genome Res*, 2012; 22(9): 1775–89
4. Spizzo R, Almeida MI, Colombatti A et al: Long non-coding RNAs and cancer: A new frontier of translational research. *Oncogene*, 2012; 31(43): 4577–87
5. Yang L, Duff MO, Graveley BR et al: Genomewide characterization of non-polyadenylated RNAs. *Genome Biol*, 2011; 12(2): R16
6. Caley DP, Pink RC, Trujillano D et al: Long noncoding RNAs, chromatin, and development. *ScientificWorldJournal*, 2010; 10: 90–102
7. Svoboda M, Slysokova J, Schneiderova M et al: HOTAIR long non-coding RNA is a negative prognostic factor not only in primary tumors, but also in the blood of colorectal cancer patients. *Carcinogenesis*, 2014; 35(7): 1510–15
8. Qiu M, Xu Y, Yang X et al: CCAT2 is a lung adenocarcinoma-specific long non-coding RNA and promotes invasion of non-small cell lung cancer. *Tumour Biol*, 2014; 35(6): 5375–80
9. Han Y, Hu H, Zhou J: Knockdown of lncRNA SNHG7 inhibited epithelial-mesenchymal transition in prostate cancer through miR-324-3p/WNT2B axis *in vitro*. *Pathol Res Pract*, 2019 [Epub ahead of print]
10. Yang E, Xue L, Li Z, Yi T: Lnc-AL445665.1-4 may be involved in the development of multiple uterine leiomyoma through interacting with miR-146b-5p. *BMC Cancer*, 2019; 19(1): 709
11. Guo F, Fu Q, Wang Y, Sui G: Long non-coding RNA NR2F1-AS1 promoted proliferation and migration yet suppressed apoptosis of thyroid cancer cells through regulating miRNA-338-3p/CCND1 axis. *J Cell Mol Med*, 2019; 23(9): 5907–19
12. Peng CL, Zhao XJ, Wei CC et al: LncRNA HOTAIR promotes colon cancer development by down-regulating miRNA-34a. *Eur Rev Med Pharmacol Sci*, 2019; 23(13): 5752–61
13. Iyer MK, Niknafs YS, Malik R et al: The landscape of long noncoding RNAs in the human transcriptome. *Nat Genet*, 2015; 47(3): 199–208
14. van Bakel H, Nislow C, Blencowe BJ et al: Most “dark matter” transcripts are associated with known genes. *PLoS Biol*, 2010; 8(5): e1000371
15. Mercer TR, Dinger ME, Mattick JS: Long non-coding RNAs: Insights into functions. *Nat Rev Genet*, 2009; 10(3): 155–59
16. Jia M, Jiang L, Wang YD et al: lincRNA-p21 inhibits invasion and metastasis of hepatocellular carcinoma through Notch signaling-induced epithelial-mesenchymal transition. *Hepatol Res*, 2016; 46(11): 1137–44
17. Shukla S, Zhang X, Niknafs YS et al: Identification and validation of PCAT14 as prognostic biomarker in prostate cancer. *Neoplasia*, 2016; 18(8): 489–99
18. Askarian-Amiri ME, Leung E, Finlay G et al: The regulatory role of long non-coding RNAs in cancer drug resistance. *Methods Mol Biol*, 2016; 1395: 207–27
19. Xu Y, Zhang G, Zou C et al: LncRNA MT1JP suppresses gastric cancer cell proliferation and migration through MT1JP/MiR-214-3p/RUNX3 axis. *Cell Physiol Biochem*, 2018; 46(6): 2445–59
20. Ye F, Gong Y, Chen X et al: Long noncoding AFAP1-antisense RNA 1 is up-regulated and promotes tumorigenesis in gastric cancer. *Oncol Lett*, 2018; 15(5): 7523–30
21. Liu J, Yang C, Gu Y et al: Knockdown of lncRNA SNHG8 inhibits cell growth in Epstein-Bar virus-associated gastric carcinoma. *Cell Mol Biol Lett*, 2018; 23: 17
22. Chang Y, Zhang J, Zhou C et al: Long non-coding RNA FOXD2-AS1 plays an oncogenic role in hepatocellular carcinoma by targeting miR-206. *Oncol Rep*, 2018; 40(6): 3625–34
23. Lei T, Zhu X, Zhu K et al: EGR1-induced upregulation of lncRNA FOXD2-AS1 promotes the progression of hepatocellular carcinoma via epigenetically silencing DKK1 and activating Wnt/ β -catenin signaling pathway. *Cancer Biol Ther*, 2019; 20(7): 1007–16
24. Xu K, Zhang Z, Qian J et al: LncRNA FOXD2-AS1 plays an oncogenic role in hepatocellular carcinoma through epigenetically silencing CDKN1B(p27) via EZH2. *Exp Cell Res*, 2019; 380(2): 198–204
25. Qiu F, Xiong JP, Deng J et al: TRIM functions as an oncogene in gastric cancer and is regulated by miR-185. *Int J Clin Exp Pathol*, 2015; 8(5): 5053–61
26. Tan Z, Jiang H, Wu Y et al: miR-185 is an independent prognosis factor and suppresses tumor metastasis in gastric cancer. *Mol Cell Biochem*, 2014; 386(1–2): 223–31
27. Zhao L, Zhang Y, Liu J et al: MiR-185 inhibits cell proliferation and invasion of non-small cell lung cancer by targeting KLF7. *Oncol Res*, 2018 [Epub ahead of print]
28. Zhang W, Sun Z, Su L et al: miRNA-185 serves as a prognostic factor and suppresses migration and invasion through Wnt1 in colon cancer. *Eur J Pharmacol*, 2018; 825: 75–84
29. Xia D, Li X, Niu Q et al: MicroRNA-185 suppresses pancreatic cell proliferation by targeting transcriptional coactivator with PDA-binding motif in pancreatic cancer. *Exp Ther Med*, 2018; 15(1): 657–66
30. Lin Z, He R, Luo H et al: Integrin-beta5, a miR-185-targeted gene, promotes hepatocellular carcinoma tumorigenesis by regulating beta-catenin stability. *J Exp Clin Cancer Res*, 2018; 37(1): 17
31. Tsitoura E, Wells AU, Karagiannis K et al: MiR-185/AKT and miR-29a/collagen 1a pathways are activated in IPF BAL cells. *Oncotarget*, 2016; 7(46): 74569–81
32. Dong H, Cao W, Xue J: Long noncoding FOXD2-AS1 is activated by CREB1 and promotes cell proliferation and metastasis in glioma by sponging miR-185 through targeting AKT1. *Biochem Biophys Res Commun*, 2019; 508(4): 1074–81
33. Zhang X, Zhang HM: Alantolactone induces gastric cancer BGC-823 cell apoptosis by regulating reactive oxygen species generation and the AKT signaling pathway. *Oncol Lett*, 2019; 17(6): 4795–802
34. Zhang L, Lian R, Zhao J et al: lGFBP7 inhibits cell proliferation by suppressing AKT activity and cell cycle progression in thyroid carcinoma. *Cell Biosci*, 2019; 9: 44

Conclusions

The results in our study demonstrated that FOXD2-AS1 knock-out could effectively increase the expression of miR-185, thus inhibiting the expression of AKT and p-AKT protein entering nuclei, which inhibits the biological activity of Bel-7402 cells.